Mineralogical Magazine, August 1999, Vol. 63(4), pp. 489–501

Two contrasting mineral assemblages in the Meliata blueschists, Western Carpathians, Slovakia

S. W. FARYAD[1] AND G. HOINKES[2]

[1,2]Institute of Crystallography, Mineralogy and Petrology, University of Graz, Universitätplatz 2, 0811 Graz, Austria
[1,]*Department of Geology and Mineralogy, Technical University Košice, Letná 9, 04200 Košice, Slovakia.

ABSTRACT

Low-grade metamorphic rocks from the Meliata unit (Western Carpathians) are characterized by the presence of typical blueschist-facies minerals. In metabasalt, an early low-pressure assemblage (<0.5 GPa at 350°C), characterized by muscovite and zoisite, is followed by high-pressure glaucophane, phengite, Na-pyroxene, chlorite, clinozoisite and Al-poor titanite, indicating pressures of >1.2 GPa at 450°C. Na-pyroxene shows strong compositional variations between the end-members Jd_{4-70}, Aeg_{10-49} and Q_{17-49}, respectively. Phengite has high Si content of 3.5 a.p.f.u. The zoisite with Al_2Fe ($100[Fe_{tot}/(-2+Al_{tot}+Fe_{tot})]$) = 3–5%, is rimmed by clinozoisite, with a maximum of 75% Al_2Fe, as well as being enclosed by glaucophane. The occurrence of clinozoisite, rimming zoisite, suggests that the transformation of orthorhombic to monoclinic epidote depends not only on the temperature but also on the pressure. In the studied metabasalt, retrograde phases reflecting greenschist-facies conditions are albite and chlorite. Some neighbouring metabasites may additionally contain actinolite and biotite.

KEYWORDS: zoisite-clinozoisite, muscovite-phengite, omphacite, prograde metamorphism, Meliata unit.

Introduction

THE most common minerals in blueschist-facies metabasites are glaucophane, albite and lawsonite/epidote (Ernst, 1971; Black, 1977; Maruyama and Liou, 1988). Depending on the whole-rock composition and *P-T* conditions, some metabasites may contain pumpellyite, actinolite, phengite, garnet or Na-rich clinopyroxene (hereafter referred to as sodic pyroxene). The Fe^{3+}- and Al-rich varieties of sodic pyroxene are widespread in blueschist-facies rocks, whereas, the Na-Ca (Mg,Fe^{2+}) variety, omphacite usually appears only at eclogite or at the transition to eclogite-facies conditions. It may coexist with zoisite/clinozoisite, paragonite or kyanite (Selverstone, 1984; Miller, 1990; Ghent and Stout, 1994). The sodic pyroxenes already reported in metabasites and phyllites from the Meliata unit (Fig. 1) are mostly aegirine augite, aegirine and jadeite (Jd <53%), coexisting with blue amphibole, albite and epidote ± garnet (Faryad, 1995*a*,*b*). A compositionally heterogeneous sodic pyroxene of aegirine augite-omphacite-jadeite composition, associated with glaucophane, clinozoisite and phengite has been observed in a metabasalt also containing relict muscovite, paragonite and zoisite. This is the first record of omphacite in the Meliata blueschists, in the form of crystals with zones of unusual compositions. The occurrence of two potassic white micas and two epidote group minerals in this rock suggest a multistage metamorphic evolution, to be extended to the whole Meliata blueschist unit. Besides the possible influence of pressure on zoisite-clinozoisite transformation, these contrasting mineral assemblages are discussed in the present paper, in order to reconstruct the *P-T* path history of the Meliata blueschists.

Outline of the geology and petrology of blueschists

The Meliata unit, occurring in the southern part of the Western Carpathians (Fig. 1), represents an

---

* Address for correspondence

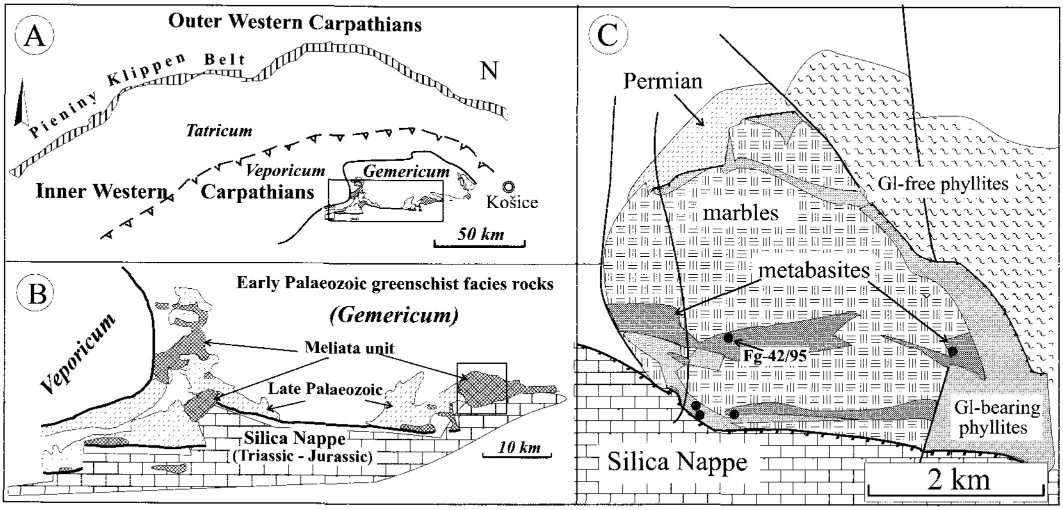

FIG. 1. Geological map indicating the position of the Meliata unit in the frame of the Western Carpathians (A, B) and the location of pyroxene-bearing metabasites and phyllites (C).

accretionary complex containing very low-grade metamorphic carbonate and clastic sediments together with tectonic fragments and slices of serpentinites and blueschist-facies metamorphic rocks (Reichwalder, 1973; Hovorka *et al.*, 1985; Faryad, 1995*a,b*; Kozur and Mock, 1996). The blueschist-facies metamorphism is interpreted as the result of the southvergent subduction of the Triassic Meliata-Hallstatt oceanic basin crust and nearby continental wedge rocks, including the Western Carpathian basement units (Faryad and Henjes-Kunst, 1997). The most common blueschist-facies rocks exposed at the surface are marbles which are intercalated with metabasalts and phyllites. Besides serpentinites, these rock sequences are assumed to represent an oceanic suite, since metabasites have compositions comparable to those of transitional MORB-arc basalts. Rocks of continental affinity, also affected by high-pressure metamorphism, correspond to quartz conglomerates, older amphibolite facies rocks, metabasites and mica schists that contain early Palaeozoic mica (Faryad and Henjes-Kunst, 1997).

Metabasites associated with marbles contain blue amphibole, albite, epidote, titanite, phengite, quartz and one or more of the following minerals: garnet, Na-pyroxene, paragonite, chlorite and actinolite. Besides quartz and phengite, the phyllitic rocks may contain paragonite, chlorite, chloritoid, garnet and Na-pyroxene. From the composition of coexisting minerals, a prograde metamorphism from 0.8 GPa/300°C to 1.2 GPa/450°C has been assumed by using the advanced versions of Ge0-Calc and Thermocalc programs (Faryad, 1995*a*) based on thermodynamic datasets of Berman (1988) and of Holland and Powell (1990). Retrograde metamorphism is documented by the appearance of actinolite, albite, biotite and chlorite. K-Ar and Ar-Ar phengite ages indicated a middle Jurassic age for the high-pressure metamorphic event (Maluski *et al.*, 1993; Dallmayer, 1994; Faryad and Henjes-Kunst, 1997).

The Na-pyroxene was found in only three metabasite and two phyllite samples (Fig. 1*c*). In metabasites it occurs as: (1) pseudomorphs after igneous diopsidic augite; (2) rims of diopsidic augite; (3) individual tabular crystals; and (4) fine-grained aggregate in the matrix. The first two modes of occurrence are found in relatively coarse-grained metabasite with a well-preserved gabbro texture (Faryad, 1995*a,b*). The latter two modes of occurrence, which are discussed in the present paper, were found in a metabasalt with a fine-grained matrix (sample Fg-42/95). This metabasalt contains lithoclasts of relatively coarse-grained mafic rock, which also contain Na-pyroxene. Compared to other metabasites, also intercalated in marbles, this rock shows high MgO, Al_2O_3 and low FeO_t contents (Fig. 2). The whole-rock analysis and estimated mineral mode are given in Table 1.

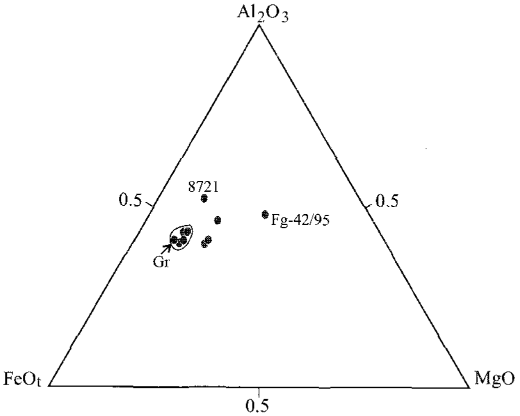

FIG. 2. Whole-rock Al_2O_3:FeO_t:MgO ratios in the Meliata blueschist-facies metabasites, forming layers in marbles or occurring adjacent to them. Samples Fg-42/95 and 8721 contain Na-pyroxene with high a jadeite content. Gr indicates samples with garnet.

TABLE 1. Major oxide contents (in wt.%) and estimated mineral mode in metabasalt of sample Fg-42/95

SiO_2	47.60	Gl	15–25%
TiO_2	0.60	Na-Cpx	15–25%
Al_2O_3	18.50	Zo	5–15%
Fe_2O_3	6.32	Cz	1–5%
FeO	3.30	Chl	5–15%
MnO	0.01	Ph	5–15%
MgO	10.32	Ms	1–5%
CaO	6.50	Tnt	1–5%
Na_2O	2.08	Prg	<1%
K_2O	0.52	Ab	1–5%
P_2O_5	0.20	Ap	<1%
H_2O^+	3.87	Mt	<1%
		Hem	<1%
Total	99.82		

Gl – glaucophane, Cpx – pyroxene, Zo – zoisite, Chl – chlorite, Ph – phengite, Ms – muscovite, Tnt – titanite, Prg – paragonite, Ab – albite, Ap – apatite, Mt – magnetite, Hem – hematite.

Textural relations

In the studied metabasalt (sample Fg-42/95), the fine-grained matrix and the small lithoclasts (1 × 2 cm in size) of relatively coarse-grained rock consist of Na-pyroxene, glaucophane, phengite, zoisite-clinozoisite, titanite and chlorite. Accessory magnetite mostly replaced by hematite, and apatite also occur in this sample. The fine-grained matrix, formed by Na-pyroxene and phengite with small amounts of chlorite and titanite, is represented by the presence of relatively large (up to 1 mm in length) tabular idiomorphic pseudomorphs of phengite with small amounts of titanite (Fig. 3*a*). These are formed by the replacement of individual or intergrown crystals. Phengite, together with zoisite-clinozoisite, occurs also as vein-shaped segregations in which radial phengite crystals are oriented perpendicular to the vein wall. These veins are cross-cut by pyroxene and glaucophane. Two varieties of chlorite can be distinguished in the matrix. Accessory amounts of tabular chlorite (I) form mono-mineral aggregates that may contain zoisite, rimmed by clinozoisite (Fig. 4). Chlorite (II) replaces glaucophane or pyroxene. The fine-grained matrix, including the pseudomorphs filled by phengite, is crossed by long (up to 3 mm) crystals of glaucophane.

The coarse-grained lithoclasts contain more phengite, chlorite and zoisite-clinozoisite. Na-pyroxene forms tabular grains (0.5–1.0 mm in size) and may contain inclusions of columnar-shaped pseudomorphs, consisting of phengite and small amounts of chlorite. Contact zones between Na-pyroxene and zoisite are usually formed by chlorite and phengite, but zoisite cross-cut by Na-pyroxene or forming inclusions with the pseudomorphs in Na-pyroxene (Fig. 3*b*) was also observed. Back-scattered electron images indicate muscovite, paragonite and titanite inclusions in zoisite. Two textural varieties of glaucophane can be distinguished. Accessory glaucophane (I) occurs as inclusions in Na-pyroxene (Fig. 5). Most glaucophane (II), similar to that in the fine-grained matrix, cross-cuts the Na-pyroxene and phengite pseudomorphs, whereas it encloses zoisite-clinozoisite crystals (Fig. 6).

In conclusion, three stages of metamorphism, identified by specific assemblages, have been observed: (1) zoisite with inclusions of muscovite, paragonite and some titanite represents relict phases (assemblage 1) which were formed during an early stage of metamorphism. (2) The blueschist-facies assemblage (assemblage 2) is represented by Na-pyroxene, glaucophane, phengite, clinozoisite-epidote and titanite in the matrix, or forming inclusions in glaucophane and Na-pyroxene. Both glaucophane and Na-pyroxene contain inclusions of zoisite which

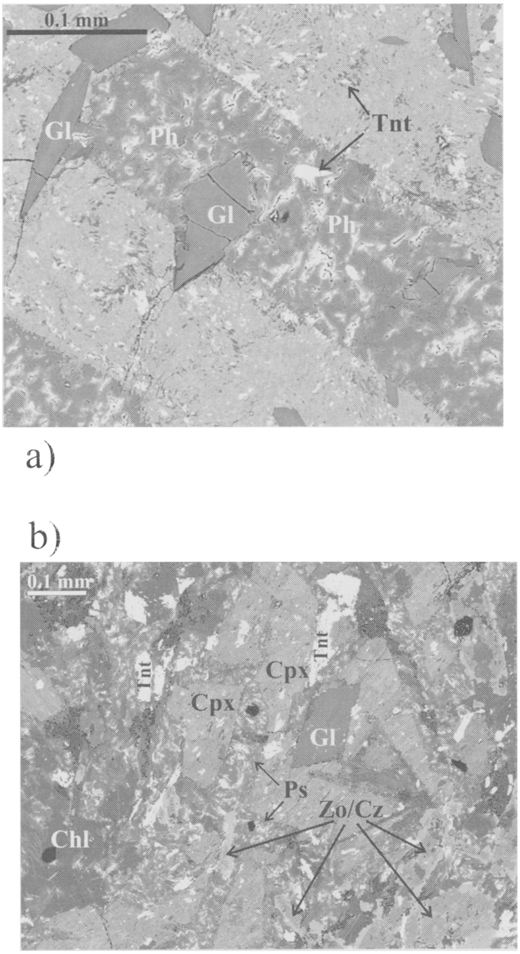

FIG. 3. Pseudomorphs of phengite in fine-grained matrix (*a*) and enclosed in pyroxene (*b*) in metabasalt (Fg-42/95). The fine-grained matrix consists of Na-pyroxene with small amounts of titanite, chlorite, albite and phengite. The pseudomorphs are crossed by glaucophane. Psedomorphs of phengite (Ps) enclosed in pyroxene also contain chlorite. Zo/Cz shows zoisite rimmed by clinozoisite occurring in or adjacent to pyroxene and pseudomrphs.

belong to assemblage (I). Some mono-mineralic aggregates of chlorite (I), cross-cut by glaucophane also seem to be at equilibrium with blueschist-facies minerals. (3) The minerals formed during the retrograde stage (assemblage 3) are chlorite (II) and albite, replacing Na-pyroxene and glaucophane.

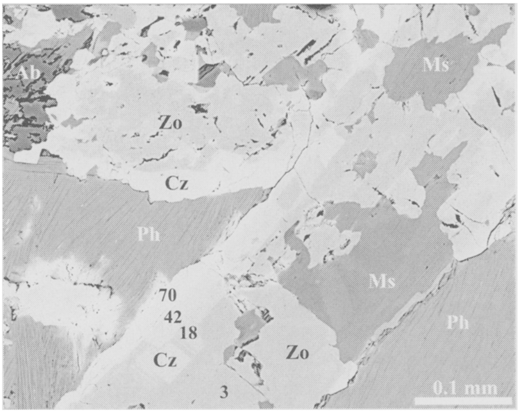

FIG. 4. Zoisite crystals, rimmed by clinozoisite (back-scattered electron image) in phengite (a) Numbers indicate mol.% Al_2Fe in zoisite and in clinozoisite.

Mineral chemistry

Most minerals were analysed with a scanning electron microscope JEOL 6310 with wavelength- and energy-dispersive spectrometers at the Institute for Mineralogy, Crystallography and Petrology in Graz. The standards were pyrope (Mg, Al), adularia (K), rutile (Ti), tephroite (Mn), jadeite (Na, Si) and andradite (Fe, Ca). The operating voltage was 15 kV. Beam currents were 10 or 15 nA with 20 s counting time. The mineral formulae and the ferric and ferrous iron ratios were calculated using the methods given in Tables 2–6.

Sodic pyroxene

The fine-grained sodic pyroxene in the matrix is mostly aegirine augite and omphacite with average contents of the three end-members Jd_{30}, Aeg_{34} and Q_{37} (Q = Wo + En + Fs) (Table 2). Large Na-pyroxene crystals reveal strong irregular zoning which can easily be observed by back-scattered electron imagery (Fig. 5). The jadeite-rich domains of the BSE image are characterized by dark grey spots in pale grey sodic pyroxene crystals of omphacite or aegirine compositions. Some of these jadeite-rich domains are columnar-shaped (Fig. 5), and probably originated from the replacement of an Al-rich phase. Compositional variation between Jd_{4-70}, Aeg_{15-49}, Q_{15-49} may be found in a single sodic pyroxene crystal. Figure 7 shows the composi-

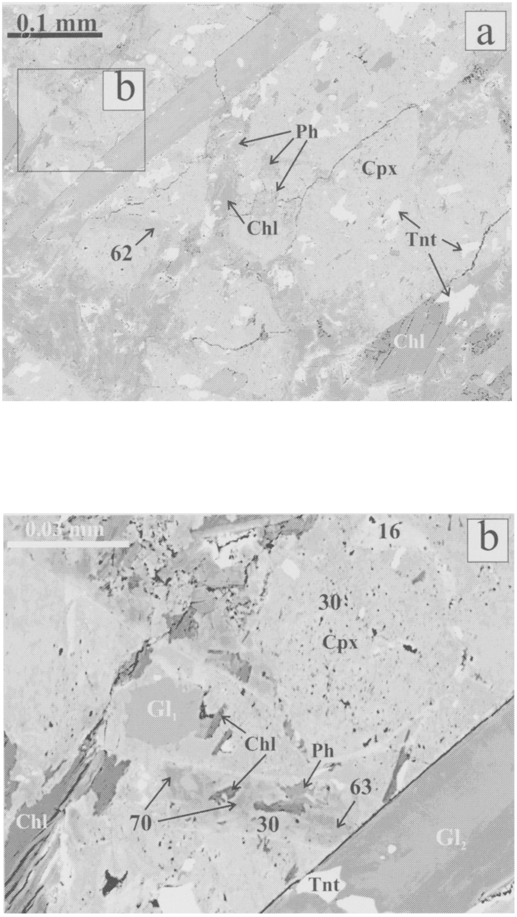

FIG. 5. Back-scattered electron image of Na-pyroxene with pseudomorphs of chlorite and phengite. Columnar forms correspond to Na-pyroxene domains, rich in jadeite contents. Numbers indicate mol.% jadeite in Na-pyroxene. Gl_1 is Ca-rich glaucophane enclosed in pyroxene. Gl_2 is glaucophane crossing Na-pyroxene.

tional range of sodic pyroxene from two other metabasite samples from the Meliata unit. In contrast to those samples, where aegirine or aegirine augite dominate, the sodic pyroxene from sample Fg-42/95 has a composition corresponding to aegirine augite-omphacite-jadeite (Jd_{4-70}, Aeg_{49-18}, Q_{47-12}.

Amphiboles

Throughout the whole unit, the blue amphiboles are of glaucophane, and only some Fe-rich varieties may contain riebeckite (Faryad, 1995*a*). They largely reveal a prograde chemical zonation with an Al-poor core and an Al-rich rim. In sample Fg-42/95, the two textural varieties of glaucophane are different in composition. Glaucophane (Gl_1), enclosed in Na-pyroxene (Fig. 5), has a high Mg content with average $X_{Mg} = 0.8$ and $X_{Al} = (Al/(Al{+}Fe^{3+}) = 0.7$ (Table 3). The most common glaucophane (Gl_2) which cross-cuts Na-pyroxene (Fig. 5) or encloses zoisite-clinozoisite has lower CaO (0.4–1.2 wt.%) and higher Al_2O_3 (6.7–10.3 wt.%) contents compared to glaucophane Gl_2 (CaO = 2.3–2.5 and Al_2O_3 = 6.3 wt.%). Large Gl_2 amphibole crystals indicate a weak prograde zonation with decreasing CaO and FeO_t and increasing Al_2O_3 contents towards the rims.

Zoisite-clinozoisite

Columnar crystals (up to 0.5 mm in length) of epidote group minerals, which may form inclusions in glaucophane or in pyroxene, were optically identified as zoisite. Optically, these crystals appear homogeneous, but compositional variation was found in all crystals by means of back-scattered electron images (Fig. 4). The zoisite crystals of assemblage I are rimmed by clinozoisite, which together with small clinozoisite-epidote grains in the matrix belongs to assemblage (II). Representative analyses of zoisite and clinozoisite are given in Table 4. The mol.% of $Al_2Fe = 100[Fe_{tot}/(-2+Al_{tot}+Fe_{tot})]$ in zoisite is 3–5%. The Al_2Fe content in clinozoisite is 16–80 mol.%. Clinozoisite with maximum Al_2Fe content occurs in the matrix without zoisite core or forms the outermost zone of zoisite rim.

White micas

Based on textural relations and chemical compositions, several varieties of white mica have been distinguished in sample Fg-42/95. White micas, enclosed in zoisite correspond to muscovite with a Si content of 3.0 a.p.f.u. and occasionally also to paragonite (Table 5). Four textural varieties of white mica: (1) fine-grained, occurring with omphacite and chlorite in the matrix; (2) filling pseudomorphs after idiomorphic forms; (3) radial, occurring in veins; and (4) forming inclusions in titanite, are of phengite with a Si content of 3.4–3.5 a.p.f.u.

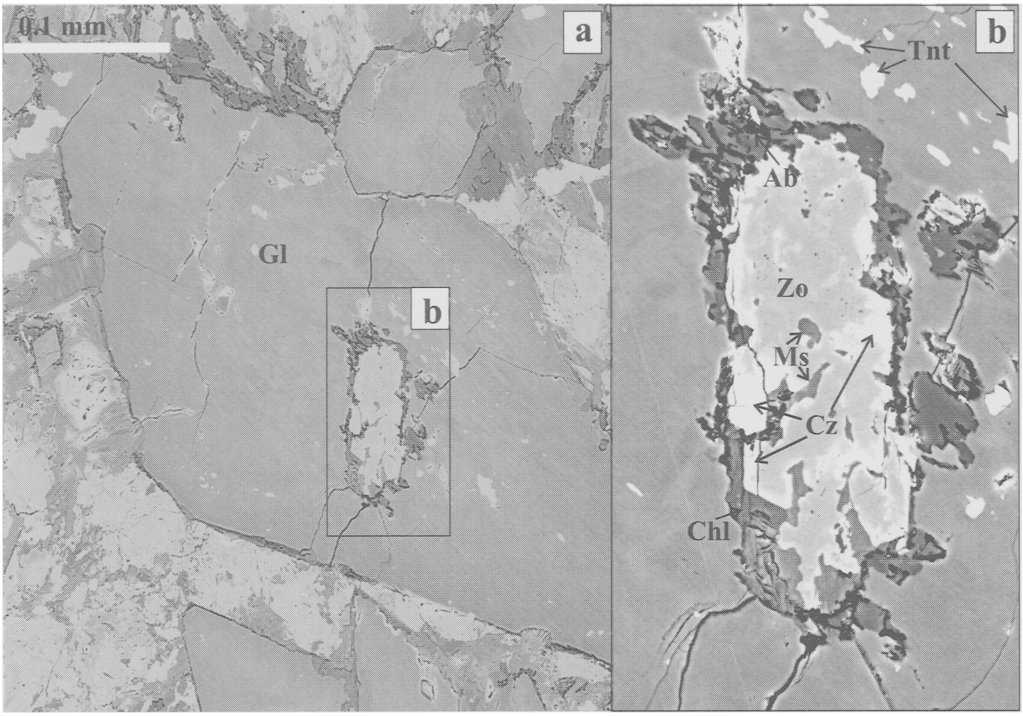

FIG. 6. Back-scattered electron image of glaucophane enclosing zoisite, rimmed by clinozoisite. The zoisite contains inclusions of muscovite. The boundary between clinozoisite and glaucophane is formed by retrograde chlorite and albite.

Chlorite

All textural varieties of chlorite (I) and (II) are rich in Mg with $X_{Mg} = 0.79-0.81$ (Table 6). No clear variation was found in different occurrences of chlorite.

Titanite

Titanite is common both as inclusions in zoisite, Na-pyroxene and glaucophane, and also in the fine-grained matrix. Some large titanite crystals enclose phengite. The titanite found in the matrix and which forms inclusions in Na-pyroxene and amphibole, when analysed, indicates no regular zoning and the Al_2O_3 content is ~1 wt.% (Table 6). Titanite with a greater Al_2O_3 content, up to 6.4 wt.% is present as inclusions in zoisite.

Discussion and tectonic implication

The presence of relatively coarse-grained lithoclasts in a fine-grained matrix suggests that the protolith of the blueschists was a basalt or basaltic tuff. This interpretation is supported by the geological observation that the metabasite layers have a gradual transition to marbles (Reichwalder, 1973; Faryad, 1995*a*). Cracks, filled by phengite and zoisite in the metabasalt (sample Fg-42/95), reflect the static characteristics of an early stage of metamorphism. Regarding the muscovite inclusions in zoisite, the phengite filling veins had to be formed by transformation of an earlier muscovite.

Nature of the pseudomorphs

Since no relic was found in the pseudomorphs filled by phengite, the primary phase remains unclear. The sharp contacts of pseudomorphs with fine-grained Na-pyroxene in the matrix as well as with tabular shaped Na-pyroxene suggest that the primary phase was in equilibrium with Na-pyroxene. Pseudomorphs after lawsonite are common in high-temperature blueschists and in low-temperature eclogites, but they usually

TABLE 2. Representative microprobe analyses of Na-clinopyroxene in sample Fg-42/95

Form	Tabular grains				Fine-grained	
An. no.	3-9	2-9	3-6	2-1	matrix	matrix
SiO_2	56.68	56.18	56.31	55.19	54.45	54.41
TiO_2	0.14	0.08	0.36	0.00	0.06	0.31
Al_2O_3	16.87	16.77	16.99	6.92	6.75	7.20
Fe_2O_3	3.57	7.36	4.18	9.78	11.67	16.43
FeO	2.86	0.82	2.67	1.73	3.10	0.89
MnO	0.12	0.00	0.02	0.12	0.08	0.22
MgO	3.30	1.98	3.52	7.89	5.25	3.34
CaO	4.20	3.26	4.46	10.81	8.52	6.38
Na_2O	11.56	12.97	11.65	7.97	8.54	10.51
K_2O	0.01	0.02	0.02	0.04	0.07	0.00
Total	99.31	99.44	100.18	100.45	98.49	99.69
Si	1.993	1.981	1.970	1.991	2.016	1.997
Al^{IV}	0.007	0.019	0.030	0.009	0.000	0.003
Al^{VI}	0.687	0.688	0.670	0.285	0.294	0.219
Ti	0.004	0.002	0.010	0.000	0.002	0.009
Fe^{3+}	0.094	0.195	0.110	0.266	0.325	0.454
Fe^{2+}	0.084	0.024	0.078	0.052	0.096	0.027
Mn	0.004	0.000	0.001	0.004	0.003	0.007
Mg	0.173	0.104	0.184	0.424	0.290	0.183
Ca	0.158	0.123	0.167	0.418	0.338	0.251
Na	0.794	0.887	0.790	0.558	0.613	0.748
K	0.001	0.001	0.001	0.002	0.004	0.000
Aegirine	0.094	0.190	0.109	0.262	0.32	0.460
Jadeite	0.694	0.682	0.674	0.290	0.297	0.298

Normalization on the basis of 12 charges and Fe^{3+} = aegirine
Analyses 3-9, 2-9 and 3-6 are from idiomorphic domains of pyroxene (Fig. 5*c*).

contain clinozoisite or other Ca-bearing phase (Miller, 1990). With the exception of titanite, no other Ca-bearing phase has been found in the pseudomorphs of the present study. Rectangular-shaped phengite pseudomorphs, similar to lawsonite, may occur in some blueschist-facies phyllites of the Meliata unit. Similarly, in the metabasites these pseudomorphs do not contain a Ca-bearing phase. Assuming that the phengite pseudomorphs in the metabasalt matrix (Fig. 3*a*) are after lawsonite, then the columnar phengite aggregates in sodic pyroxene (Fig. 3*b*) could also be formed after lawsonite. The mono-mineralic aggregates of chlorite (I), containing zoisite crystals and crossed by glaucophane can be interpreted as pseudomorphs after an igneous pyroxene (amphibole?) or may represent filling of amygdales in a basaltic matrix.

Determination of metamorphic P-T *conditions*

The three mineral assemblages described in the previous sections reflect three different metamorphic stages, which occurred at different metamorphic conditions.

Stage I (Zo + Ms + Prg + Al-Tnt)

A low-temperature limit of 300°C/0.3 GPa–340°C/0.5 GPa for the formation of zoisite is considered by extrapolation of the lawsonite-zoisite transformation reaction Lws + Ab = Prg + Zo + Qtz + W (Fig. 8) (Heinrich and Althaus, 1988). The *P-T* conditions for muscovite and paragonite formation can be estimated by calculation of the sliding reaction (1) 5 Cel + 6 Prg = Clin + 5 Ms + Ab + 2 Qtz + 2 H_2O (Fig. 8) based on the thermodynamic datasets of Berman

TABLE 3. Representative microprobe glaucophane analyses from sample Fg-42/95

An. no.	Gl_1		Gl_2 1c	1r	2c	2r
SiO_2	56.72	56.57	56.17	59.19	58.02	58.43
TiO_2	0.12	0.21	0.02	0.02	0.02	0.06
Al_2O_3	6.77	6.32	7.25	8.66	6.74	10.31
Fe_2O_3	9.83	6.77	6.77	5.01	6.46	4.07
FeO	2.34	4.72	4.34	5.29	5.63	5.06
MnO	0.21	0.20	0.22	0.15	0.34	0.16
MgO	13.22	13.27	12.93	12.48	12.58	12.57
CaO	2.27	2.38	1.07	0.57	1.22	0.43
Na_2O	6.52	5.97	6.43	7.24	6.64	7.09
K_2O	0.00	0.02	0.07	0.02	0.01	0.00
Total	98.00	96.43	95.27	98.63	97.66	98.18
Si	7.800	7.909	7.909	7.999	8.002	7.896
Al^{IV}	0.200	0.091	0.091	0.001	0.000	0.104
Al^{VI}	0.900	0.950	1.110	1.379	1.095	1.537
Ti	0.012	0.022	0.002	0.002	0.002	0.006
Fe^{3+}	1.018	0.712	0.718	0.510	0.670	0.414
Fe^{2+}	0.269	0.551	0.511	0.598	0.650	0.572
Mn	0.025	0.023	0.027	0.018	0.039	0.018
Mg	2.710	2.765	2.714	2.514	2.586	2.531
Ca	0.334	0.357	0.162	0.083	0.180	0.063
Na^{M4}	1.737	1.619	1.756	1.896	1.776	1.859
Na	0.000	0.000	0.000	0.003	0.000	0.000
K	0.000	0.003	0.012	0.002	0.002	0.000
X_{Mg}	0.910	0.834	0.842	0.807	0.799	0.815

Cations calculated on the basis of 23 oxygens and 15 cations + K
c – core, r – rim

(1988) and the new version of the Ge0-calc program, distributed by Berman in 1992. Because of the lack of equilibrium chlorite in the assemblage (I), the reaction (1) was calculated for different chlorite compositions. The results of this calculation (Fig. 8) show small pressure variations of 3.8–4.2 GPa at 320–340°C for chlorite with X_{Mg} = 0.8–0.5.

Stage 2 (Na-Cpx + $Gl_{I,2}$ + Ph + Cz + Tnt + Chl_I)

Although glaucophane cross-cuts the Na-pyroxene, all these phases are at equilibrium. A weak zonation in glaucophane (Gl_2) caused mainly by a lower Ca content compared to that in glaucophane (Gl_1) enclosed in Na-pyroxene, suggests an increase of pressure during metamorphism. This prograde increase of pressure can be assumed from textural relations, since Ca-rich glaucophane forms inclusions in Na-pyroxene. Strong compositional variation and irregular zoning of Na-pyroxene which are visible in back-scattered electron images (Fig. 5) seem to be a result of local equilibrium and replacement of an older phase, or they may represent jadeite-rich crystals formed at relatively low temperature. Assuming a maximum temperature of 460°C which was calculated by different geothermometric methods for this part of the Meliata blueschists (Faryad, 1995*a,b*), a minimum pressure of 1.2 GPa can be considered from the maximum jadeite content (70 mol.%), using the Ab = Jd+Q (Holland and Powell, 1996) and Ab = Jd-Aeg+Q (Liu and Bohlen, 1995) barometers. Pressures of >1.2 GPa at 460°C are derived also by the Si isopleths of Massonne and Schreyer (1978). From equilibrium curve (2) Cel + 4 Qtz + 4 Jd = Ms + 2 Gl + 2 H_2O (Fig. 8), calculated using the average jadeite composition in the Na-pyroxene of Jd_{40}, a pressure of ~13 kbar at 460°C can be estimated.

TABLE 4. Representative microprobe analyses of epidote group minerals in sample Fg-42/95

	Zoisite					Clinozoisite	
	c	c	cr	r	r	r	matrix
SiO_2	39.23	39.35	38.01	39.01	38.49	37.19	37.38
TiO_2	0.11	0.02	0.31	0.01	0.14	0.01	0.10
Al_2O_3	32.80	33.00	31.52	31.77	27.83	23.29	23.23
Fe_2O_3	0.46	0.54	2.92	3.38	7.00	13.24	13.28
MnO	0.04	0.01	0.54	0.04	0.25	0.00	0.07
MgO	0.11	0.23	0.18	0.10	0.00	0.14	0.00
CaO	25.17	25.32	24.10	24.04	23.51	22.52	23.61
Na_2O	0.06	0.01	0.05	0.04	0.04	0.03	0.03
K_2O	0.07	0.04	0.10	0.00	0.00	0.00	0.00
Total	98.05	98.52	97.73	98.39	97.26	96.42	97.7
Si	2.985	2.980	2.927	2.973	3.011	3.002	2.988
Ti	0.006	0.001	0.018	0.001	0.008	0.001	0.006
Al	2.942	2.946	2.861	2.854	2.566	2.215	2.188
Fe^{3+}	0.027	0.030	0.169	0.194	0.412	0.804	0.799
Mn	0.003	0.000	0.032	0.002	0.015	0.000	0.004
Mg	0.013	0.026	0.020	0.011	0.000	0.017	0.000
Ca	2.052	2.055	1.989	1.963	1.970	1.947	2.022
Na	0.009	0.002	0.008	0.005	0.007	0.004	0.005
K	0.007	0.004	0.010	0.000	0.000	0.000	0.000
Al_2Fe	2.8	3.1	16.4	18.4	42.1	78.8	80.9

Cations calculated on the basis of 12 oxygens and 1 OH-group

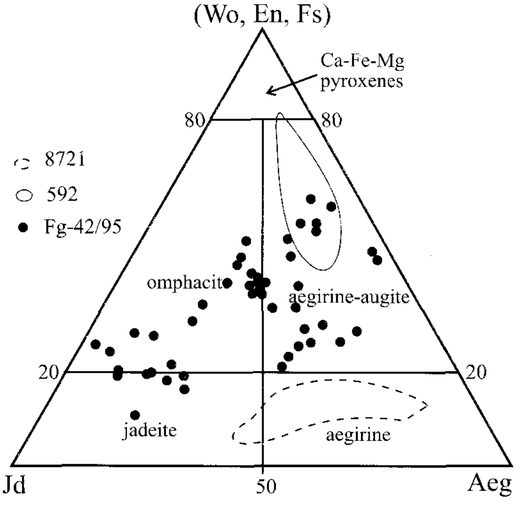

FIG. 7. Q-Jd-Aeg diagram of Morimoto (1988) for Na-pyroxenes from three metabasite samples from the Meliata unit.

Two alternative *P-T* paths for prograde metamorphism from stage 1 (<5 kbar) to stage 2 (>12 kbar) are inferred from the nature and interpretation of pseudomorphs of phengite. Considering that the pseudomorphs are after lawsonite, the *P-T* path overstepped the lawsonite-zoisite boundary reaction at lower pressure and returned to the zoisite/clinozoisite field near peak pressure conditions (Fig. 8). If the pseudomorphs were formed by the replacement of a phase other than lawsonite, then the pressure increased from greenschist- to blueschist-facies conditions in the zoisite/clinozoisite stability field.

Stage 3 (Ab + Chl_2)

Chlorite and albite, replacing glaucophane and pyroxene are retrograde phases formed at greenschist-facies conditions at <0.8 GPa and <400°C. Some metabasites in the studied locality, in addition to chlorite and albite, also contain biotite, which replaces garnet or glaucophane (Faryad, 1995) and may suggest temperatures of >300°C.

TABLE 5. Representative microprobe analyses of micas from sample Fg-42/95

Mica	Muscovite		Paragonite		Phengite				
included	in Zo		in Zo		in Cpx	in pseudomorphs			in Tnt
SiO_2	46.34	46.53	45.55	46.57	53.43	53.55	53.96	53.29	51.22
TiO_2	0.05	0.23	0.00	0.00	0.24	0.00	0.03	0.26	0.26
Al_2O_3	39.39	39.58	41.00	41.83	23.74	23.48	24.05	24.43	22.48
Fe_2O_3	0.54	0.37	0.18	0.23	2.21	2.66	2.47	1.34	3.12
FeO	0.00	0.00	0.00	0.00	0.00	0.10	0.00	1.10	0.00
MnO	0.00	0.03	0.06	0.00	0.14	0.00	0.04	0.12	0.04
MgO	0.16	0.32	0.00	0.24	5.24	4.80	5.08	4.52	6.94
CaO	0.11	0.25	0.55	0.46	0.13	0.16	0.13	0.08	0.13
Na_2O	0.38	1.10	6.59	6.55	0.15	0.16	0.13	0.68	0.11
K_2O	10.34	9.72	0.86	1.18	9.56	10.47	10.40	10.57	9.37
Total	97.31	98.13	94.79	97.06	94.84	95.38	96.29	96.39	93.67
Si	2.975	2.966	2.906	2.899	3.516	3.551	3.527	3.512	3.391
Ti	0.002	0.011	0.000	0.000	0.012	0.000	0.002	0.013	0.013
Al	2.981	2.973	3.083	3.068	1.841	1.836	1.853	1.897	1.754
Fe^{3+}	0.026	0.018	0.009	0.011	0.110	0.133	0.122	0.067	0.155
Fe^{2+}	0.000	0.000	0.000	0.000	0.000	0.006	0.000	0.061	0.000
Mn	0.000	0.002	0.003	0.000	0.008	0.000	0.002	0.007	0.002
Mg	0.016	0.030	0.000	0.023	0.514	0.475	0.495	0.444	0.685
Ca	0.008	0.017	0.038	0.031	0.009	0.011	0.009	0.005	0.009
Na	0.047	0.136	0.815	0.790	0.019	0.021	0.016	0.087	0.014
K	0.847	0.790	0.070	0.093	0.803	0.886	0.867	0.889	0.791

Cations calculated on the basis of 11 oxygens and 6 cations + Na + K + Ca

Zoisite/clinozoisite relations

By studying zoisite-clinozoisite from different metamorphic rocks, Enami and Banno (1980) found that the compositional gap between these two epidote minerals shifts towards the Fe^{3+}-rich side with an increase of temperature. The dependence on temperature of the presence of Fe^{3+} in zoisite-clinozoisite, was confirmed by Prunier and Hewitt (1985). These authors assumed that pressure has no influence on the transformation of zoisite to clinozoisite, because of the very small differences in their molar volume. Franz and Selverstone (1992) used an empirical phase diagram for the transformation of orthorhombic to monoclinic epidote minerals and found that pressure should have a significant effect on the position and shape of the two phase region. Textural and phase relations in sample Fg-42/95, shown mainly by the presence of muscovite inclusions in zoisite and the coexistence of clinozoisite with glaucophane, phengite and Na-pyroxene, are in agreement with the suggestion by Franz and Selverstone (1992) that zoisite and clinozoisite formation occurs at low and high-pressure conditions, respectively.

Conclusions

Zoisite and omphacite occurring in the Meliata blueschist were formed at different metamorphic conditions. Low-pressure conditions of <0.5 GPa/350°C are assumed for muscovite-zoisite-paragonite and Al-rich titanite formation. Clinozoisite, rimming zoisite or occurring in the fine-grained matrix, was formed by increasing temperature but also at pressures which led to the appearance of glaucophane, phengite and Na-pyroxene. This finding indicates a pressure dependence of the zoisite-clinozoisite transformation, agreeing with the observations of Franz and Selverstone (1992). The presence of two textural varieties of glaucophane (Gl_1 and Gl_2) with different Ca contents or a decrease of Ca towards the rims in Gl_2 suggest a progressive increase of pressure during metamorphism. However, the whole-rock

TABLE 6. Representative analyses of chlorite and titanite from sample Fg-42/95

	Chlorite			Titanite				
position	in Cpx	in matrix	aggr-Zo	in Zo		in Cpx	in Chl	in Cpx
SiO_2	30.00	31.20	29.77	31.12	31.47	30.37	30.39	31.37
TiO_2	0.00	0.00	0.13	33.65	31.60	38.34	39.82	38.53
Al_2O_3	17.85	19.55	18.89	4.28	6.03	1.61	0.84	1.10
Fe_2O_3	0.00	0.00	0.00	0.71	0.17	0.18	0.00	0.56
FeO	10.16	10.56	10.46	0.92	1.37	0.63	0.40	0.00
MnO	0.38	0.32	0.25	0.14	0.01	0.01	0.00	0.14
MgO	27.00	25.72	26.37	0.53	0.44	0.09	0.07	0.00
CaO	0.16	0.28	0.11	27.26	27.30	27.95	27.62	28.85
Na_2O	0.01	0.04	0.03	0.02	0.07	0.01	0.12	0.11
K_2O	0.04	0.23	0.02	0.04	0.03	0.00	0.00	0.05
Total	85.6	87.9	86.03	98.67	98.49	99.19	99.26	100.71
Si	5.979	6.096	5.918	1.004	1.008	0.992	0.996	1.008
Ti	0.000	0.000	0.019	0.816	0.761	0.942	0.981	0.931
Al	4.194	4.502	4.427	0.163	0.227	0.062	0.032	0.042
Fe^{3+}	0.000	0.000	0.000	0.017	0.004	0.005	0.000	0.014
Fe^{2+}	1.694	1.726	1.740	0.025	0.037	0.017	0.011	0.000
Mn	0.064	0.053	0.042	0.004	0.000	0.000	0.000	0.004
Mg	8.023	7.491	7.814	0.026	0.021	0.004	0.004	0.000
Ca	0.035	0.059	0.024	0.942	0.937	0.978	0.969	0.993
Na	0.002	0.015	0.011	0.002	0.004	0.001	0.008	0.007
K	0.009	0.057	0.005	0.002	0.001	0.000	0.000	0.002

Chlorite: calculated on the basis of 20 cations and 28 oxygens
Titanite: calculated on the basis of 3 cations and 10 charges – OH-group
aggr-Zo aggregate with zoisite (Fig. 4*b*)

composition of sample Fg-42/95 (higher Al_2O_3 content compared with other metabasites of the Meliata unit) and the high jadeite content of Na-pyroxene were controlled by the composition of local domains in the rocks. The Al-rich domains of sodic pyroxene are probably either the result of local equilibrium after an Al-rich phase, or represent jadeite crystals later enclosed by omphacite or aegirine. Minimum pressure of 1.2 GPa at 450°C for the Meliata unit is assumed from the high jadeite content in Na-pyroxene. The two contrasting mineral assemblages in the Meliata unit with *P-T* conditions of <0.5 GPa/350°C and >1.2 GPa/450°C, respectively, suggest a high subduction rate following a very steep geotherm of oceanic and continental rocks.

Acknowledgements

This work was supported by the Austrian Research Fund through project M417-GEO, awarded to S.W.F., by a Lise Meitner Fellowship (1997–1998), and by the Slovak Academic Agency (project VEGA-1/5003/98). The first author thanks K. Ettinger for his introduction to the quantitative scanning electron microscopy methods. J.L.R. Touret and A.M. Clark are thanked for their thoughtful review and helpful comments on the manuscript.

References

Black, P.M. (1977) Regional high-pressure metamorphism in New Caledonia: phase equilibria in the Ouégoa District. *Tectonophys.*, **43**, 89–107.

Berman, R.G. (1988) Internally-consistent thermodynamic data for minerals in the system Na_2O-K_2O-CaO-MgO-FeO-Fe_2O_3-Al_2O_3-SiO_2-TiO_2-H_2O-CO_2. *J. Petrol.*, **29**, 445–522.

Dallmeyer, R.D., Neubauer, F., Fritz, H. and Putis, M. (1994) Variscan vs. Alpine tectonothermal evolution within the Eastern Alps and Western Carpathians, Austria-Slovakia. *J. Czech Geol. Soc.*, **39**, 120–1.

Enami, M. and Banno, S. (1980) Zoisite-clinozoisite relations in low- to medium-grade high-pressure metamorphic rocks and their implications. *Mineral.*

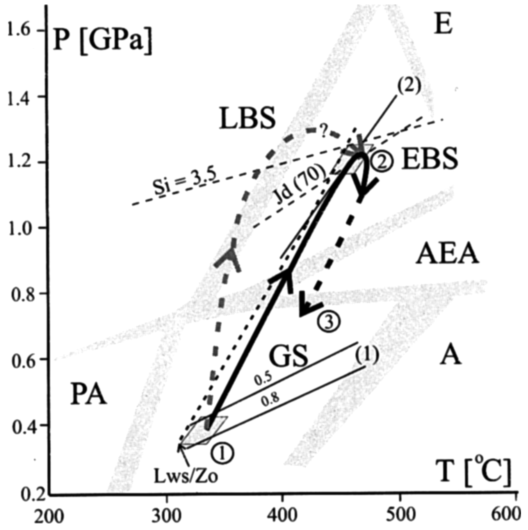

FIG. 8. The *P-T* path for the Meliata blueschist-facies rocks, inferred from two contrasting assemblages: Ms + Zo + Prg (lower box) and Ph + Cz + Gl + Na-Cpx (upper box). Numbers 1–3 in circles correspond to three metamorphic stages as indicated in the text. The grey dashed line represents an alternative *P-T* path assumed by phengite pseudomorphs after lawsonite (see text). The sliding reactions (1 and 2) were calculated using the thermodynamic detasets of Berman (1988) and the program Ge0-Calc (Berman, 1992): (1) 5 Cel + 6 Prg = Clin + 5 Ms + Ab + 2 Qtz + 2 H_2O; and (2) Cel + 4 Qtz + 4 Jd = Ms + 2 Gl + 2 H_2O. The numbers 0.5 and 0.8 correspond to nX_{Mg} values of chlorite used in reaction (1). Reactions Lws/Zo - 4 Lws + Ab = Prg + 2 Zo + 2 Qtz + 6 H_2O and 4 Lws + Jd = Prg + 2 Zo + Qtz + 6 H_2O are from Heinrich and Althous (1988). The metamorphic facies (PA – pumpellyite-actinolite, LBS – lawsonite blueschist, EBS – epidote blueschist, AEA – albite-epidote amphibolite, A – amphibolite and GS – greenschist) are after Evans (1990). The mineral symbols, other than Cel = Al-celadonite, Clin = clinochlore, Lws = lawsonite and Jd = jadeite are as used in Table 1. Isopleths of Si are after (Massonne and Schreyer, 1987). Ab = Jd (70) + Qtz is taken from Holland and Powell (1996).

Mag., **3**, 1005–13.

Ernst, G. (1971) Do mineral parageneses reflect unusually high-pressure conditions of the Franciscan metamorphism? *Amer. J. Sci.*, **270**, 81–108.

Evans, B.W. (1990) Phase relations of epidote-blueschists. *Lithos*, **25**, 3-23.

Faryad, S.W. (1995*a*) Phase petrology and P-T conditions of mafic blueschists from the Meliata unit, Western Carpathians, Slovakia. *J. Metam. Geol.*, **13**, 701–14.

Faryad, S.W. (1995*b*) Petrology and phase relations of low-grade high-pressure metasediments from the Meliata unit, Western Carpathians, Slovakia. *Eur. J. Mineral.*, **7**, 71–87.

Faryad, S.W. and Henjes-Kunst, F. (1997) K-Ar and Ar-Ar age constraints of the Meliata blueschist facies rocks, the Western Carpathians (Slovakia). *Tectonophys.*, **280**, 141–56.

Franz, G. and Selverstone, J. (1992) An empirical phase diagram for the clinozoisite-zoisite transformation in the system $Ca_2Al_3Si_3O_{12}(OH)$-$Ca_2Al_2Fe^{3+}$-$Si_3O_{12}(OH)$. *Amer. Mineral.*, **77**, 631–42.

Ghent, E.D. and Stout, M.Z. (1994) Geobarometry of low-temperature eclogites: applications of isothermal pressure-activity calculations. *Contrib. Mineral. Petrol.*, **116**, 500–7.

Heinrich, W. and Althaus, E. (1988) Experimental determination of the reactions 4 Lws + Ab = Prg + 2 Zo + 2 Qtz + 6 W and 4 Lws + Jd = Prg + 2 Zo + Qtz + 6 W. *Neues Jahrb. Mineral. Abh.*, **11**, 516–28.

Holland, T.J.B and Powell, R. (1990) An enlarged and updated internally consistent thermodynamic dataset with certainties and correlations: the system K_2O-Na_2O-CaO-MgO-MnO-FeO-Fe_2O_3-Al_2O_3-TiO_2-SiO_2-C-H_2-O_2. *J. Metam. Geol.*, **8**, 89–124.

Holland, T. and Powell, R. (1996) Thermodynamics of order-disorder in minerals: II. Symmetric formalism applied to solid solution. *Amer. Mineral.*, **81**, 1425–37.

Hovorka, D., Ivan, P., Jaroš, J., Kratochviíl, M., Reichwalder, P., Rojkovič, I. Spišiak, J. and Turanová, L. (1985) *Ultramafic Rocks of the Western Carpathians, Czechoslovakia.* Geol. Inst. Dionýz Štúr, Bratislava, 258 p.

Kozur, H. and Mock, R. (1996) New paleogeographic and tectonic interpretations in the Slovakian Carpathians and their implications for correlations with the Eastern Alps. Part I: Central Western Carpathians. *Mineralia Slovaca*, **28**, 151–74.

Liu, J. and Bohlen, S.R. (1995) Mixing properties and stability of jadeite-acmite pyroxene in the presence of albite and quartz. *Contrib. Mineral. Petrol.*, **119**, 433–40.

Maluski, H., Rajlich, P. and Matte, Ph. (1993) $^{40}Ar/^{39}Ar$ dating of the Inner Carpathian Variscan Basement and Alpine mylonitic overprinting, *Tectonophys.*, **223**, 313–37.

Maryuama, S. and Liou, J. (1988) Petrology of Franciscan metabasites along the jadeite-glaucophane type facies series, Cazdero, California. *J. Petrol.*, **29**, 1–37.

Massonne, H.J. and Schreyer, W. (1987) Phengite geobarometry based on the limiting assemblage with K-feldspar, phlogopite, and quartz. *Contrib. Mineral. Petrology*, **96**, 212–24.

Miller, Ch. (1990) Petrology of type locality eclogites from the Korealpe and Saualpe (Eastern Alps), Austria. *Schweiz. Mineral. Petrogr. Mitt.*, **70**, 287–300.

Morimoto, N. (1988) Nomenclature of pyroxenes. *Schweiz. Mineral. Petrogr. Mitt.*, **68**, 95–111.

Prunier, A.R and Hewitt, D.A. (1985) Experimental observations on coexisting zoisite-clinozoisite, *Amer. Mineral.*, **70**, 375–8.

Reichwalder, P. (1973) Geologische Verhältnisse des jüngeren Paläozoikums im Süd Teil des Zips-Gemerer Erzgebirges. *Západné Karpaty*, **18**, 99–139, Geol. Inst. D. Štúr, Bratislava.

Selverstone, J., Spear, F.S., Franz, G. and Morteani, G. (1984) High-pressure metamorphism in the SW Tauern Window, Austria: P-T paths from hornblende-kyanite-staurolite schists. *J. Petrol.*, **25**, 501–31.

[*Manuscript received 11 February 1998: revised 18 November 1998*]